Classification of renal tumour using convolutional neural networks to detect oncocytoma

Pedersen, Mikkel; Andersen, Michael Brun; Christiansen, Henning; Asawi, Nessn H.

Published in:
European Journal of Radiology

DOI:
10.1016/j.ejrad.2020.109343

Publication date:
2020

Document Version
Peer reviewed version

Citation for published version (APA):
Pedersen, M., Andersen, M. B., Christiansen, H., & Asawi, N. H. (2020). Classification of renal tumour using convolutional neural networks to detect oncocytoma. *European Journal of Radiology*, *133*(109343), [109343]. https://doi.org/10.1016/j.ejrad.2020.109343

Classification of Renal Tumour Using Convolutional Neural Networks to Detect Oncocytoma

Mikkel Pedersen (Methodology) (Software) (Validation) (Formal analysis) (Investigation) (Data curation) (Writing - original draft) (Writing - review and editing), Michael Brun Andersen (Methodology) (Validation) (Investigation) (Resources) (Writing - original draft) (Writing - review and editing), Henning Christiansen (Methodology) (Software) (Validation) (Formal analysis) (Data curation) (Writing - original draft) (Writing - review and editing), Nessn H. Azawi (Conceptualization) (Methodology) (Validation) (Investigation) (Resources) (Writing - original draft)<ce:contributor-role>Writing - review and editing, Supervision, Project administration)

PII: S0720-048X(20)30532-5

DOI: https://doi.org/10.1016/j.ejrad.2020.109343

Reference: EURR 109343

To appear in: *European Journal of Radiology*

Received Date: 23 July 2020

Revised Date: 29 September 2020

Accepted Date: 5 October 2020

Please cite this article as: Pedersen M, Andersen MB, Christiansen H, Azawi NH, Classification of Renal Tumour Using Convolutional Neural Networks to Detect Oncocytoma, *European Journal of Radiology* (2020), doi: https://doi.org/10.1016/j.ejrad.2020.109343

Classification of Renal Tumour Using Convolutional Neural Networks to Detect Oncocytoma

Mikkel Pedersen, Michael Brun Andersen, Henning Christiansen, Nessn H. Azawi

Mikkel Pedersen: Department of People and Technology (DPT), Roskilde University Universitetsvej 1, 4000 Roskilde. mikkped@ruc.dk

Michael Brun Andersen: Department of Radiology, Herlev-Gentofte University Hospital, Herlev Ringvej 75, 2700 Herlev. E-mail: michael.brun.andersen@regionh.dk

Henning Christiansen: Department of People and Technology (DPT), Roskilde University Universitetsvej 1, 4000 Roskilde. Phone: +45 46 74 38 32. E-mail: henning@ruc.dk

Nessn H. Azawi: Department of Urology, Zealand University Hospital, Department of Clinical Medicine, Copenhagen University. Roskilde, Sygehusvej 10, 4000 Roskilde. Tel: +45 26393034, E-mail: nesa@regionsjaelland.dk

Corresponding author

Associate professor

Nessn H. Azawi:

Department of Urology, Zealand University Hospital,

Department of Clinical Medicine, Copenhagen University.

Roskilde, Sygehusvej 10, 4000 Roskilde.

Tel: +45 26393034, E-mail: nesa@regionsjaelland.dk

Abstract

Purpose

To investigate the ability of convolutional neural networks (CNNs) to facilitate differentiation of oncocytoma from renal cell carcinoma (RCC) using non-invasive imaging technology.

Methods

Data were collected from 369 patients between January 2015 and September 2018. True labelling of scans as benign or malignant was determined by subsequent histological findings post-surgery or ultrasound-guided percutaneous biopsy. The data included 20,000 2D CT images.

Data were randomly divided into sets for training (70%), validation (10%) and independent testing (20%, DataTest_1). A small dataset (DataTest_2) was used for additional validation of the training model. Data were divided into sets at the patient level, rather than by individual image. A modified version of the ResNet50V2 was used. Accuracy of detecting benign or malignant renal mass was evaluated by a 51% majority vote of individual image classifications to determine the classification for each patient.

Results

Test results from DataTest_1 indicate an area under the curve (AUC) of 0.973 with 93.3% accuracy and 93.5% specificity. Results from DataTest_2 indicate an AUC of 0.946 with 90.0% accuracy and 98.0% specificity when evaluation is performed image by image.

There is no case in which multiple false negative images originate from the same patient. When evaluated with 51% majority of scans for each patient, the accuracy rises to 100% and the incidence of false negatives falls to zero.

Conclusion

CNNs and deep learning technology can classify renal tumour masses as oncocytoma with high accuracy. This diagnostic method could prevent overtreatment for patients with renal masses.

Abbreviations

Convolutional Neural Networks (CNN)

Renal cell carcinoma (RCC)

Ultrasound (US)

Computed tomography (CT)

Interquartile range (IQR)

Kilo voltage (kV)

Area under the curve (RUC)

Keywords: Deep learning, Machine learning, Oncocytoma, Renal cell carcinoma

Introduction

The past two decades have seen an increase in diagnosed renal cell carcinomas (RCC) due to incidental detection of small renal tumours resulting from increased use of computed tomography (CT) scanning [1,2]. Most enhancing renal masses observed in adults are in fact RCCs; however, a significant proportion of such masses are benign (most commonly oncocytoma). Benign tumours cannot be distinguished from malignant tumours based solely on standard imaging technology [3].

In a recent surgical series of 228 patients who underwent partial or radical nephrectomy with lesions ≤4.0 cm, 26.3% of masses were found to be benign [4,5]. The relatively high proportion of patients with benign renal cortical neoplasms who underwent surgery in this sample group highlights the important role of new diagnostic technology in preventing overtreatment.

Ultrasound-guided biopsy and computed tomography (CT)-guided biopsy are the two most commonly used methods of RCC diagnosis. The sensitivity of these methods is lower for biopsies of small masses (≤3.0 cm) than large masses (>3.0 cm) [6]. Biopsy sensitivity is limited by false negative results, which may be due either to the method's failure to properly target a small renal mass or to the insufficient presence of cells, morphological overlap or cellular heterogeneity to clarify a diagnosis. Biopsies that fail to result in a diagnosis do not necessarily indicate that a mass is benign; rather, a majority of cases reveal a malignant diagnosis in repeated biopsies [7,8]. No radiologic criteria currently exist to consistently diagnose oncocytoma due to low sensitivity and

specificity of the available biopsy technology [9]. MR and CT scans are not feasible diagnostic methodologies for oncocytoma because of overlap in the scan results of oncocytoma and RCC [10,11].

A system that enables precise automatic classification of CT images would be an important decision-making support tool for physicians providing diagnoses to their patients. In recent years, deep learning methods for convolutional neural networks (CNN) have contributed to several experiments that reported impressive results in the area of medical image analysis. Specifically, CNN and deep learning have been recognized for their ability to identify subtle yet indicative features that are difficult for the human eye to distinguish [12–15]. This study investigates the ability of a CNN to facilitate differentiation of oncocytoma from RCCs using non-invasive imaging technology.

Materials and Methods

The dataset for this study consisted of CT scans from 446 patients with an RCC or oncocytoma diagnosis. These data were extracted from a local pathological database; of the total, 67 of the scans were performed outside of the region and were therefore inaccessible, and ten of the scans were of such poor quality that the tumour could not be identified. The study sample therefore consists of 369 patient scans performed at six departments of radiology between January 2015 and September 2018. Nine of the scans were non-contrast phase only because the patients reported a contrast allergy, of them, six patients in training, two patients in DataTest_1, and one patient in validation. All patients with only non-contrast scans have had malign. The remaining scans

included a combination of non-contrast, arterial and venous phases. To ensure similarity of images, all scans were examined in the axial plane. Images were included in the analysis if they visualized a renal mass in any phase; otherwise, they were manually excluded. All scans reviewed manually by a radiologist and urologist and all scans with renal cysts or other renal lesions rather than renal tumor excluded from the cohort.The number of 2D images per patient ranged from 20–100, and the total sample consisted of more than 20,000 2D images. The slice thickness of images ranged from 1.5–5.0 mm, depending on the local radiology department protocol, and the radiation dose was 120 kilo voltage (kV) tube voltage. Original images with three colour channels of 512 x 512-pixels were downscaled to 224 x 224 by the Keras API (using the PIL package, without cropping the images) for a better fit with the ResNet network structure. True labelling of the scans as benign or malignant was determined by subsequent histological diagnosis after surgery or renal mass biopsy.

The total sample of scans was divided into categories for training (70% of scans, n = 14,001 images from 259 patients), validation to check convergence during training (10% of scans, n = 238 images from 36 patients) and (DataTest_1) for independent testing of the trained model (20% of scans, n = 948 images from 74 patients). Each of the partitions (training, validation, and test) is seen as an independent data source during training. A set of 356 images collected from 12 patients in 2019 was used independently from the primary data (DataTest_2) for additional validation of the training model. A third set of data, including 1,737 images from 37 patients who underwent surgical treatment with a histological answer of oncocytoma, were used as an independent test

(DataTest_3) to analyse the ability of a CNN to prevent overtreatment of patients with renal masses.

Random splitting of data was performed at the patient level to ensure that each group of images from an individual patient was included in the training set, one of the validation sets or one of the test sets. Following this initial categorization, each set was viewed as a collection of arbitrary images with no other patient information. Each image had a true classification as benign or malignant and there was no overlap of images from any given patient between image sets.

The study approach does not include explicit segmentation (i.e., identifying image regions that show tumours); rather, it relies on the CNN's ability to automatically identify the image features that are relevant for classification. Through training, the CNN learns to ignore anatomical features that are not related to malignancies and to add weight to features that are indicative of malignancies. The presence of a malignant tumour may create subtle changes in the surrounding anatomical structures. The CNN could theoretically add weight to those image features as well, but no evidence was found to indicate that this error occurred.

A modified version of the ResNet50V2 [16] CNN was implemented with the TensorFlow and Keras software, running on standard and affordable hardware (AMD Ryzen 2700x CPU with 16GB RAM, GeForce GTX 980ti 4GB and 1050ti 2GB GPUs).

The network hyper parameters included:

- RMSprop optimizer

- Binary Crossentropy as loss function
- Learning Rate 0.00002
- No regularization performed
- No learning rate decay introduced
- Ten epochs of training.
- All weights were trainable during training and fine-tuning of the network.

Quick convergence was expected due to the use of the RMSprop [17,18] loss optimization algorithm because averaged gradients were used. Therefore, a maximum of 20 epochs per network were trained prior to selection of the hyper parameters. Ten epochs were trained in the final model, because initial testing suggested that there were too many oscillations when more than ten epochs were trained without a decay applied to the learning rate.

ResNet50V2 classifies images into multiple categories according to the object depicted; however, this study required a simple binary classification of benign or malignant. The final connected network layers could therefore be simple, and the convolutional layers were reused. Transferred learning from ResNet50V2 was used [19]; in other words, pre-trained weights from Imagenet were applied because the initial weights for the convolutional layers and the fully connected layers for classification needed to be trained from nothing.

The accuracy for classifying a renal mass as benign or malignant was determined by a majority vote of individual image classifications. A 51% majority was used to determine each individual patient classification.

This adaptation of ResNet50V2 was trained using 70% of the data, validated using 10% of the data, and tested using 20% of the data. As described above, a patient partitioning scheme was used rather than image partitioning. Neither phasic nor serial information from the renal CT images were used in the training, validation or test data; thus, single images were classified without relation to other images from the same patient. Therefore, mixed types of phasic images could be considered independently of one another. Furthermore, the network's dense layers were simplified to reduce the chance of gaining bias or encoding of the image information into the network weights as opposed to learning features.

As it appears above, we consider patients as our datapoints rather than the total amount of images. This is apparent in our method for dividing images into training, validation and test data sets and in our adaptation of ResNet50V2; see Figure 1 and [20] for more details and a comparison of the two possible methods (patients vs. images as datapoints).

The complexity of the network is reduced considerably without loosing precision by removing the phasic and sequence (series) information and explicitly creating an image-to-patient relationship via partitioning.

Results

Three hundred patients (81%) were determined to have a malignant tumour, and 69 patients (19%) were determined to have a benign tumour. The latter were oversampled in the training set to create a balanced dataset by sampling all patients in the benign training set until a 50:50 ratio was reached between benign and malignant patients. Oversampling does have the possibility of causing overtraining of the model, but any such overtraining would be shown by a large divergence of training and validation curves for accuracy and loss during training. Also, as the orientation and position of the anatomical structures doesn't change for any image (the image is always in the same orientation and position) we choose not to apply data augmentation as the augmented data wouldn't exist in the applied use case. Thirty percent of patients were male and 70% were female. The median age for patients with a benign tumour was 68 years, (Interquartile range (IQR): 61–75), and the median age for patients with a malignant tumour was 65 years (IQR: 58–73). There was no significant difference in the size of benign and malignant tumours (p=0.56). The median size of benign tumours was 40.0 mm (IQR: 23.0–54.0), and the median size of malignant tumours was 37.0 mm (IQR: 16.0–65.0). Thirty-seven of the patients with benign tumours (54%) did not have renal mass biopsy and instead underwent surgical resection (radical or partial nephrectomy) either because the tumour was more than 4.0 cm or because the patient declined renal biopsy.

The network training resulted in a quick convergence due to use of the RMSprop loss optimization algorithm and its averaged running gradients. High performance was achieved during training in both accuracy and loss within 3–4 epochs; however, there were clear oscillations and divergence of loss following the fifth epoch. Oscillations were

reduced following the eighth epoch, and signs of convergence were reduced as an increasing number of epochs were run (see Figures 2 and 3). These findings indicate that improved performance occurs if the learning rate is decayed after the fourth epoch to allow entry into a narrow minima. The fifth epoch was selected as the study model based on the convergence and minimized oscillations as discussed above.

Analysis for DataTest_1

DataTest_1 (Test data set) indicated an area under the curve (AUC) of 0.973 with 93.3% accuracy and 93.5% specificity when evaluated image by image, indicating a converged neural net (see Figure 4). Though false negatives exist in the data, they do not originate from the same patient's scans. When the data were evaluated based on a 51% majority of individual image classifications for each patient as described above, the accuracy increased to 100% with zero false negatives.

Analysis for DataTest_2

DataTest_2 was used as an external validation set of newly collected data. This data set resulted in an AUC of 0.946 with 90.0% accuracy and 98.0% specificity when evaluated image by image (see Figure 5). As in the first data set, a small number of false negatives existed, but 100% accuracy was achieved when evaluated based on a 51% majority of image classifications per patient.

Analysis for DataTest_3

DataTest_3 (Collective/Aggregate data set) was used as an extra validation set and resulted in an AUC of 0.991 with 97.1% accuracy and 100.0% specificity when evaluated image by image (see Figure 6). As in previous sets, the accuracy increased to 100% when evaluated based on a 51% majority of image classifications per patient.

Discussion

This study's findings demonstrate that it is possible to retrain ResNet50V2 and to use a CNN for automatic classification of renal tumours in multi-phasic CT images. The dataset used in this study is substantially larger than those of comparable studies, and the data used in test sets were independent of those used in training and validation sets [21,22] . In contrast to comparable studies, information about contrast phases and depth of each 2D image was discarded. This information was deemed inessential because it does not affect the accuracy of the results, and excluding this information from the data reduces the neural network complexity and thus the training time. Oversampling was used to obtain balanced training sets because there was approximately a 4:1 ratio of malignant to benign patients.

Test results verified that overtraining was reduced by randomly dividing the 2D image sets into training and validation subsets by patient basis rather than by individual image. Classification using the trained model yielded 90.0–97.7% accuracy per image, and classification was consistently 100% accurate per patient when using a 51% majority of all 2D images in a given CT-scan. Overall, the method outlined in this study holds promise as an effective and efficient decision making support tool for medical experts because it provides an instant and reliable proposed diagnosis.

The small deviation observed in the ROC curve for DataTest_2 is most likely based on variance in the data due to factors such as machine variance, patient variance or operator variance. This deviation is accounted for in the patient majority vote classification system.

Analysis of the results from DataTest_1 and external validation of newly collected data in DataTest_2 indicate that the CNN learned the features of the CT images. Its performance in these tests is a significant improvement over existing models intended to classify CT images without the use of phasic and serial information. Further, the performance of the modified ResNet50V2 under conditions of reduced complexity and numerous convolutional layers suggests that the data is feature driven requiring feature extraction to provide data for classification, rather than complexity driven which would require added complexity (dense layers with many parameters) to represent the function required for classification.

This study's use of a CNN and deep learning technology to identify benign renal tumour masses with high accuracy could lead to a revolution in the diagnostic method in diagnostic methods for RCC. The high level of accuracy achieved in DataTest_3 indicates that a CNN could be used to prevent overtreatment of patients. If the CNN system classifies a lesion as a benign renal tumour, then a biopsy can be offered to the patient to confirm the diagnosis. External validation of this algorithm using a large data set may eliminate the need for renal biopsies in the future. In the future, a web-based platform could potentially be developed to allow an urologist to upload patient data and receive an assessment of the renal mass that indicates its probability of being malignant or benign.

Running the training of the network using data augmentation (rotation/flipping) with same network structure showed a decrease of AUC to 0.63 for DataTest_1 and AUC of 0.85 for DataTest_2. Removing the oversampling and use data augmentation leads to a decrease of AUC to 0.60 for DataTest_1 and AUC of 0.56 for DataTest_2. For both tests the curve of loss and accuracy during training did not converge, (data not presented). This could suggest that the network uses complexity to represent a transformation of the image to convert it back to its original state, thus needed further complexity to get comparable results to those without data augmentation. Another area of exploration during clinical implementation and testing would be the use of brightness, saturation, and contrast data augmentation on regions of interest to normalize data for different imaging equipment or differences in imaging techniques.

The limitations of this study include the relatively small number of patients included in the sample, as well as differences in slice thickness and phase of scan images based on protocols that differ different various departments of urology. Future research would ideally include a larger dataset drawn from all Danish hospitals to provide a critical assessment of the 100% classification accuracy observed in this study. Further research could also address the potential influence of regional differences in the historical development of CT scanners. Lastly, future research could produce heatmaps of the convolutional layers to provide an understanding of the anatomical structures and feature extraction required for the model to produce its classification. Such knowledge would allow for further optimization of the model and allow imaging techniques to be developed that emphasizes the image features required of the model.

In conclusion, CNNs and deep learning technology were used to identify renal tumour masses as oncocytoma in CT images with 90.0–97.7% accuracy by image and up to 100% accuracy per patient by a majority vote of individual image classifications.

Acknowledgements

None

Funding

This research did not receive any specific grant from funding agencies in the public, commercial, or not-for-profit sectors.

CRediT statements

Term	*Authors*
Conceptualization	*Nessn H. Azawi*
Methodology	*Mikkel Pedersen, Michael Brun Andersen, Henning Christiansen, Nessn H. Azawi*
Software	*Mikkel Pedersen, Henning Christiansen*
Validation	*Mikkel Pedersen, Michael Brun Andersen, Henning Christiansen, Nessn H. Azawi*
Formal analysis	*Mikkel Pedersen, Henning Christiansen*
Investigation	*Mikkel Pedersen, Michael Brun Andersen, Nessn H. Azawi*
Resources	*Michael Brun Andersen, Nessn H. Azawi*
Data Curation	*Mikkel Pedersen, Henning Christiansen*
Writing - Original Draft	*Mikkel Pedersen, Michael Brun Andersen, Henning Christiansen, Nessn H. Azawi*
Writing - Review & Editing	*Mikkel Pedersen, Michael Brun Andersen, Henning Christiansen, Nessn H. Azawi*
Visualization	*Preparation, creation and/or presentation of the published work, specifically visualization/ data presentation*
Supervision	*Nessn H. Azawi*
Project administration	*Nessn H. Azawi*

Reference

[1] Janzen NK, Kim HL, Figlin RA, Belldegrun AS. Surveillance after radical or partial nephrectomy for localized renal cell carcinoma and management of recurrent disease. Urol Clin North Am 2003;30:843–52.

[2] Greenlee RT, Murray T, Bolden S, Wingo PA. Cancer statistics, 2000. CA Cancer J Clin 2000;50:7–33.

[3] Ljungberg B, Bensalah K, Canfield S, Dabestani S, Hofmann F, Hora M, et al. EAU Guidelines on Renal Cell Carcinoma: 2014 Update. Eur Urol 2015;67:913–24. https://doi.org/10.1016/j.eururo.2015.01.005.

[4] Schachter LR, Cookson MS, Chang SS, Smith JA, Dietrich MS, Jayaram G, et al. Second prize: frequency of benign renal cortical tumors and histologic subtypes based on size in a contemporary series: what to tell our patients. J Endourol 2007;21:819–23. https://doi.org/10.1089/end.2006.9937.

[5] Lindkvist Pedersen C, Winck-Flyvholm L, Dahl C, Azawi NH. High rate of benign histology in radiologically suspect renal lesions. Dan Med J 2014;61:A4932.

[6] Herts BR. Imaging guided biopsies of renal masses. Curr Opin Urol 2000;10:105–9.

[7] Rybicki FJ, Shu KM, Cibas ES, Fielding JR, vanSonnenberg E, Silverman SG. Percutaneous biopsy of renal masses: sensitivity and negative predictive value stratified by clinical setting and size of masses. AJR Am J Roentgenol 2003;180:1281–7. https://doi.org/10.2214/ajr.180.5.1801281.

[8] Sutherland EL, Choromanska A, Al-Katib S, Coffey M. Outcomes of ultrasound guided renal mass biopsies. J Ultrasound 2018;21:99–104. https://doi.org/10.1007/s40477-018-0299-0.

[9] Haifler M, Copel L, Sandbank J, Lang E, Raz O, Leibovici D, et al. Renal oncocytoma--are there sufficient grounds to consider surveillance following prenephrectomy histologic diagnosis. Urol Oncol 2012;30:362–8. https://doi.org/10.1016/j.urolonc.2009.11.024.

[10] Pretorius ES, Siegelman ES, Ramchandani P, Cangiano T, Banner MP. Renal neoplasms amenable to partial nephrectomy: MR imaging. Radiology 1999;212:28–34. https://doi.org/10.1148/radiology.212.1.r99jl3228.

[11] Kay FU, Pedrosa I. Imaging of Solid Renal Masses. Urol Clin North Am 2018;45:311–30. https://doi.org/10.1016/j.ucl.2018.03.013.

[12] Sadouk L, Gadi T, Essoufi EH. A Novel Deep Learning Approach for Recognizing Stereotypical Motor Movements within and across Subjects on the Autism Spectrum Disorder. Comput Intell Neurosci 2018;2018. https://doi.org/10.1155/2018/7186762.

[13] Kosmala M, Hufkens K, Richardson AD. Integrating camera imagery, crowdsourcing, and deep learning to improve high-frequency automated monitoring of snow at continental-to-global scales. PLoS ONE 2018;13. https://doi.org/10.1371/journal.pone.0209649.

[14] Nasrullah N, Sang J, Alam MS, Mateen M, Cai B, Hu H. Automated Lung Nodule Detection and Classification Using Deep Learning Combined with Multiple Strategies. Sensors 2019;19. https://doi.org/10.3390/s19173722.
[15] Wang CJ, Hamm CA, Savic LJ, Ferrante M, Schobert I, Schlachter T, et al. Deep learning for liver tumor diagnosis part II: convolutional neural network interpretation using radiologic imaging features. Eur Radiol 2019;29:3348–57. https://doi.org/10.1007/s00330-019-06214-8.
[16] He K, Zhang X, Ren S, Sun J. Identity Mappings in Deep Residual Networks. ArXiv160305027 Cs 2016.
[17] Graves A. Generating Sequences With Recurrent Neural Networks. ArXiv13080850 Cs 2014.
[18] Tieleman T, Hinton G. Lecture 6.5-rmsprop: Divide the gradient by a running average of its recent magnitude. COURSERA Neural Netw Mach Learn 2012;4:26–31.
[19] Pedersen M, Christiansen H, Azawi NH. Efficient and Precise Classification of CT Scannings of Renal Tumors Using Convolutional Neural Networks. In: Helic D, Leitner G, Stettinger M, Felfernig A, Raś ZW, editors. Found. Intell. Syst., Cham: Springer International Publishing; 2020, p. 440–7. https://doi.org/10.1007/978-3-030-59491-6_42.
[20] Accepted Papers | ISMIS 2020 (Online Event) n.d. https://ismis.ist.tugraz.at/accepted-papers/ (accessed July 20, 2020).
[21] Han S, Hwang SI, Lee HJ. The Classification of Renal Cancer in 3-Phase CT Images Using a Deep Learning Method. J Digit Imaging 2019;32:638–43. https://doi.org/10.1007/s10278-019-00230-2.
[22] Pan T, Yang G, Wang C, Lu Z, Zhou Z, Kong Y, et al. A Multi-Task Convolutional Neural Network for Renal Tumor Segmentation and Classification Using Multi-Phasic CT Images. 2019 IEEE Int. Conf. Image Process. ICIP, 2019, p. 809–13. https://doi.org/10.1109/ICIP.2019.8802924.

Figure legends

Figure 1: Original ResNet50V2 structure compared to the version used for this study to simplify connected network layers / Conv = Convolutional, FC= fully connected (dense layer)

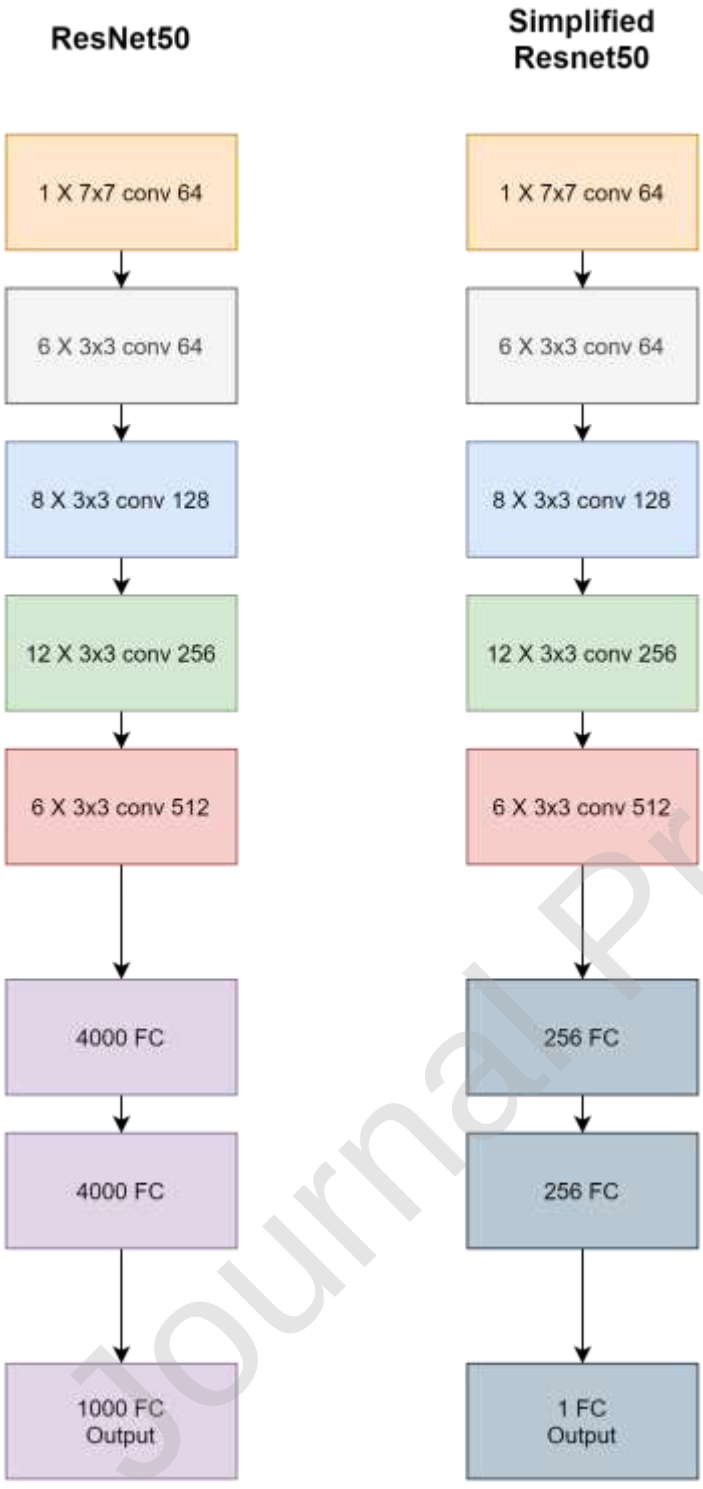

Figure 2: Quick convergence in loss curve due to RMSprop use

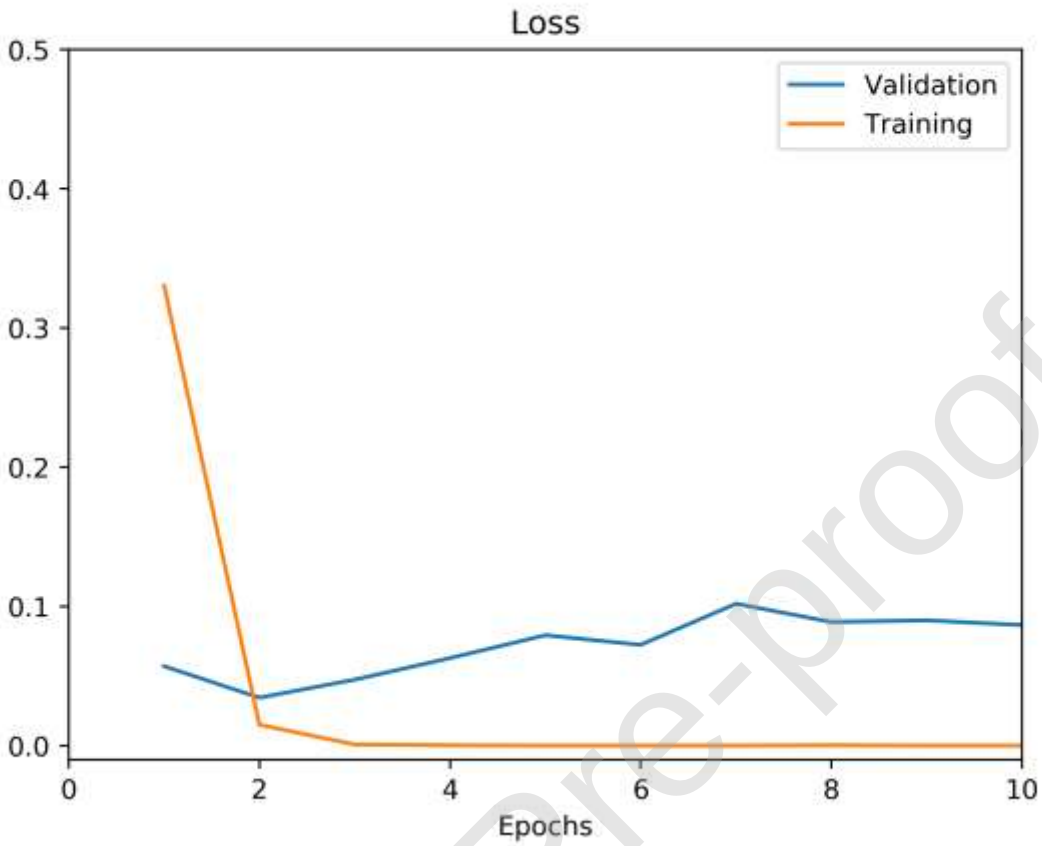

Figure 3: Quick convergence in accuracy curve due to RMSprop use

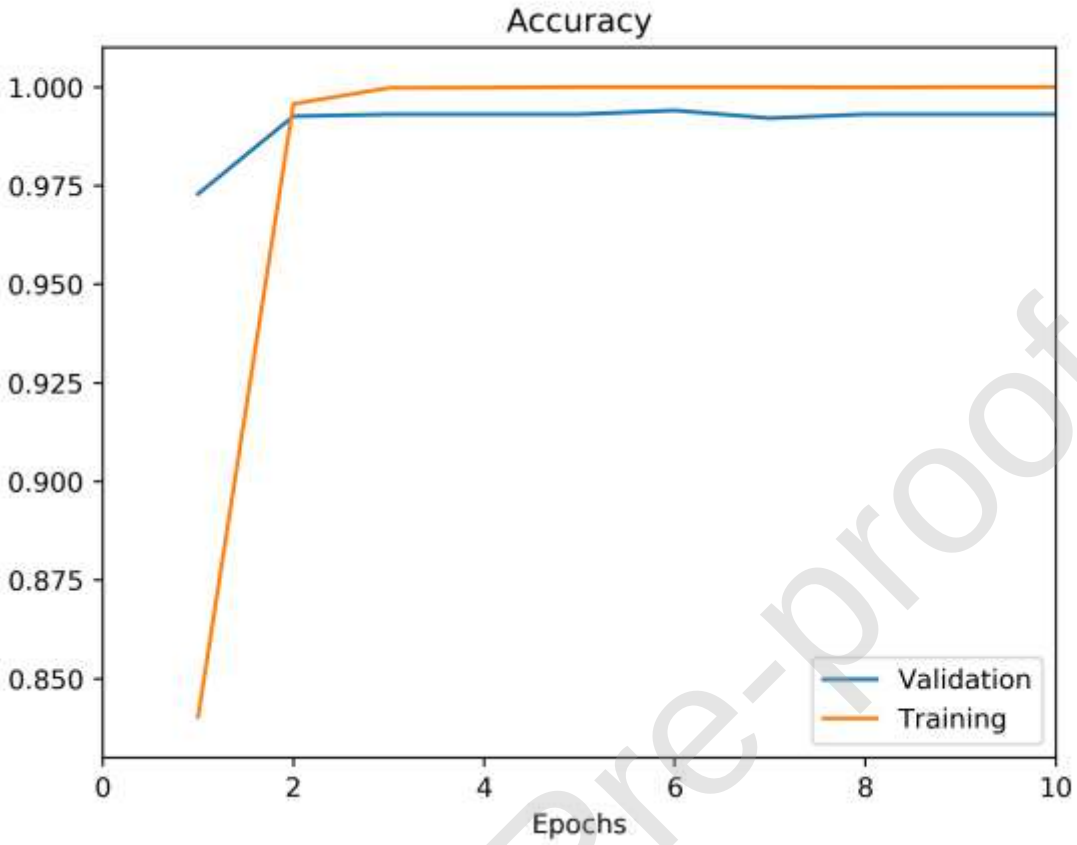

Figure 4: ROC curve analysis of DataTest_1 results when evaluated image by image

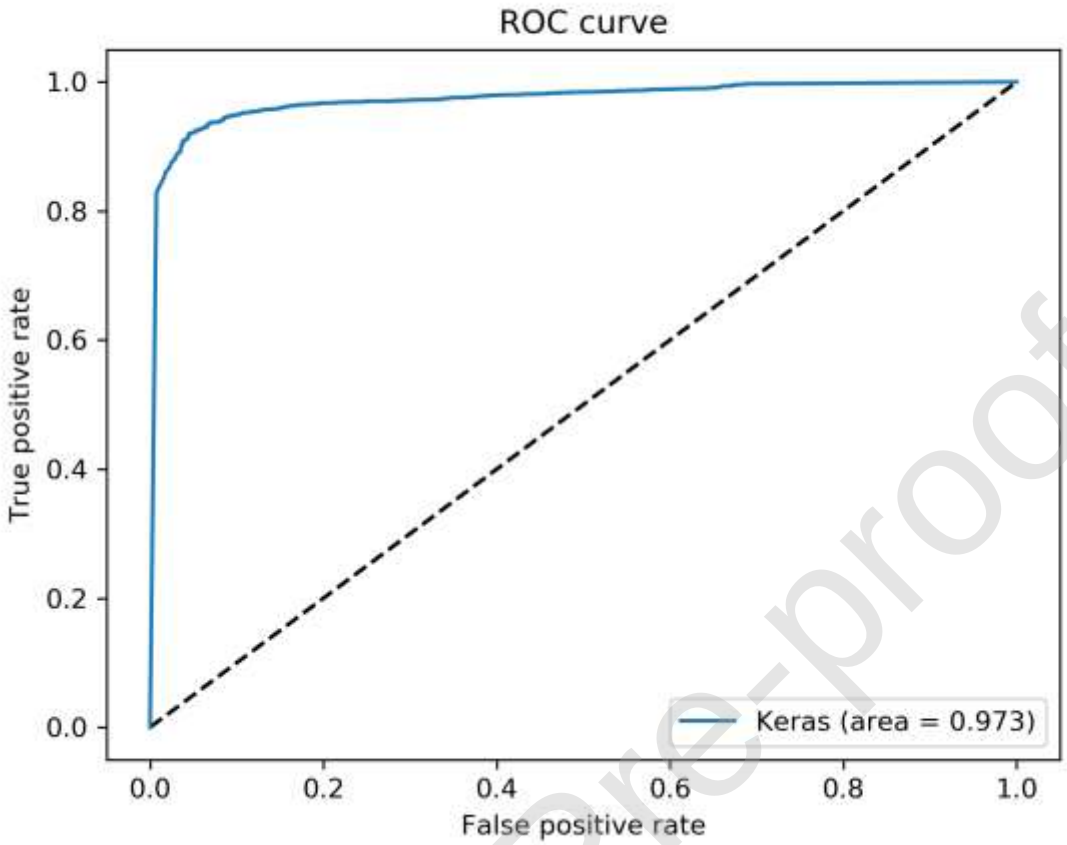

Figure 5: ROC curve analysis of DataTest_2 results when evaluated image by image

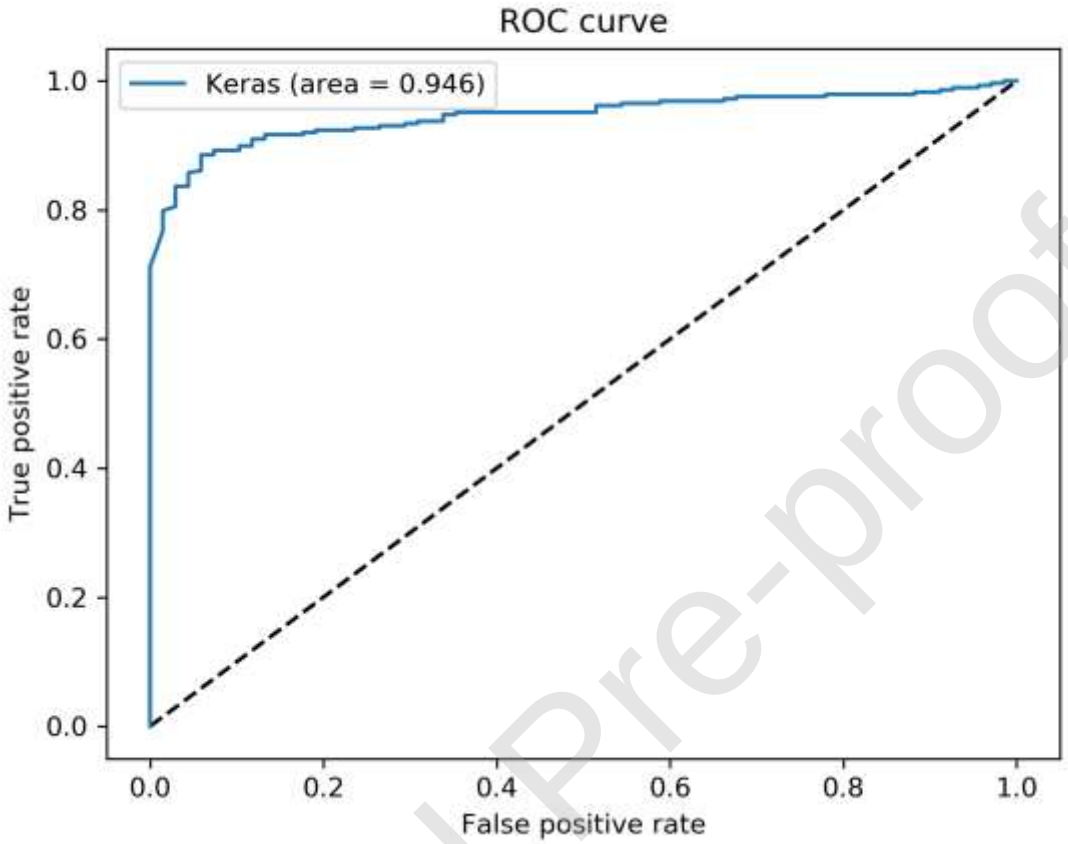

Figure 6: ROC curve analysis of DataTest_3 results when evaluated image by image